Journal Pre-proof

The Role of Natural Fe(II)-Bearing Minerals in Chemoautotrophic Chromium (VI) Bio-reduction in Groundwater

Jianping Lu (Investigation), Baogang Zhang (Conceptualization) (Supervision), Chao He (Writing - original draft), Alistair G.L. Borthwick (Writing - review and editing)

PII: S0304-3894(19)31865-5

DOI: https://doi.org/10.1016/j.jhazmat.2019.121911

Reference: HAZMAT 121911

To appear in: *Journal of Hazardous Materials*

Received Date: 2 October 2019

Revised Date: 4 December 2019

Accepted Date: 15 December 2019

Please cite this article as: Lu J, Zhang B, He C, Borthwick AGL, The Role of Natural Fe(II)-Bearing Minerals in Chemoautotrophic Chromium (VI) Bio-reduction in Groundwater, *Journal of Hazardous Materials* (2019), doi: https://doi.org/10.1016/j.jhazmat.2019.121911

The Role of Natural Fe(II)-Bearing Minerals in Chemoautotrophic Chromium (VI) Bio-reduction in Groundwater

Jianping Lu[a], Baogang Zhang[a,*], Chao He[a], Alistair G.L. Borthwick[b,c]

[a] *School of Water Resources and Environment, MOE Key Laboratory of Groundwater Circulation and Environmental Evolution, China University of Geosciences (Beijing), Beijing 100083, P. R. China*

[b] *St Edmund Hall, Queen's Lane, Oxford OX1 4AR, UK*

[c] *School of Engineering, The University of Edinburgh, The King's Buildings, Edinburgh EH9 3JL, UK*

[*]Corresponding author. Tel.: +86 10 8232 2281; Fax: +86 10 8232 1081.

E-mail: baogangzhang@cugb.edu.cn (B. Zhang).

Graphical Abstract

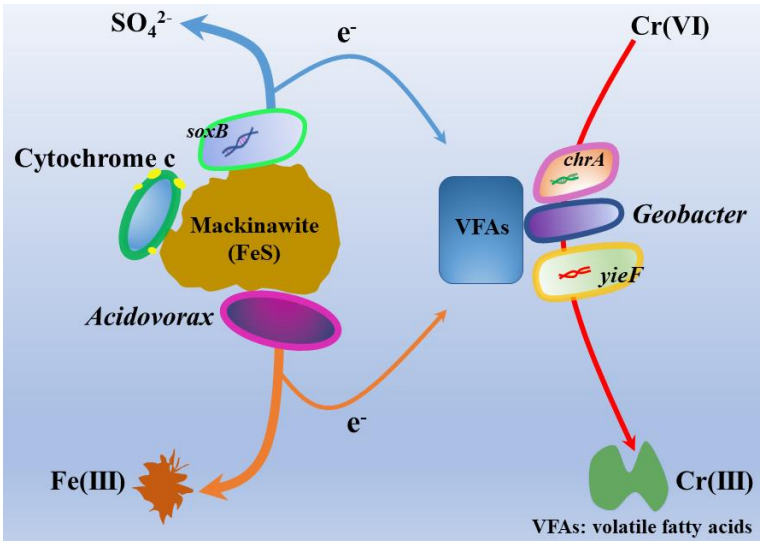

Highlights

- Fe(II)-bearing minerals can support Cr(VI) bio-reduction in groundwater.
- Mackinawite performs best in Cr(VI) removal.
- Groundwater chemistry and hydrodynamics influence the process.
- Biotic and abiotic contributions to Cr(VI) reduction are quantified.
- Synergistic mechanisms between microbial consortia are revealed.

Abstract

To date, comparatively little is known about the role of natural Fe(II)-bearing minerals in bioremediation of chromium (VI) contaminated aquifers subject to chemoautotrophic conditions. This work employed four kinds of Fe(II)-bearing minerals (pyrite, mackinawite, wustite, and magnetite) as inorganic electron donors to support Cr(VI) bio-reduction. In batch experiments, mackinawite (FeS) performed best, with Cr(VI) removal efficiency of 98.1 ± 1.21% in 96 h. Continuous column

experiments lasting 180 d implied that groundwater chemistry and hydrodynamics influenced the Cr(VI) removal process. A breakthrough study suggested that biotic and abiotic contributions to Cr(VI) reduction were 76.0 ± 1.12% and 24.1 ± 1.43%, respectively. Cr(VI) was reduced to insoluble Cr(III), whereas Fe(II) and S(-II) in mackinawite were finally oxidized to Fe(III) and sulfate. Mackinawite evolved progressively into pyrrhotite. High-throughput 16S rRNA gene sequencing indicated that mackinawite-driven Cr(VI) reduction was mediated through synergistic interactions of microbial consortia; i.e. autotrophs as *Acidovorax* synthesized volatile fatty acids as metabolic intermediates, which were consumed by Cr(VI) reducers as *Geobacter*. Genes encoding enzymes for S oxidation (*soxB*) and Cr(VI) reduction (*chrA*, *yieF*) were upregulated. Cytochrome c participating in Fe(II) oxidation increased significantly. This work advances the development of sustainable techniques for Cr(VI) polluted groundwater remediation.

Keywords: Chromium (VI); Bio-reduction; Fe(II)-bearing minerals; Mackinawite

1. Introduction

Owing to its extensive application in industry, chromium (Cr) has become widespread in the environment (Chebeir et al., 2018). There are frequent reports of groundwater contaminated by Cr. For example, aquifers in California (USA) have Cr concentration above 1 mg/L, far exceeding the state maximum contaminant level for Cr in drinking water (10 μg/L) (Hausladen et al., 2018). In Henan Province, China, groundwater from a residue-contaminated site had a Cr concentration of 164 mg/L (Huang et al., 2017). Cr usually occurs in stable oxidative state, i.e. as hexavalent Cr

(Cr(VI)) and trivalent Cr (Cr(III)) (Wang et al., 2018). Cr(VI) is a human carcinogen that causes chronic health conditions such as dermatitis, and damages organs and the human respiratory system (Liu et al., 2016). Highly toxic Cr(VI) is easily dispersed in groundwater, whereas Cr(III) tends to precipitate under alkaline conditions, with relatively low toxicity (Barrera-Diaz et al., 2012; Zhang et al., 2012).

Remediation of Cr(VI)-contaminated aquifers may be achieved through high efficiency, low cost biotransformation of Cr(VI) to Cr(III) under anaerobic conditions (Qian et al., 2017; Gang et al., 2019; Zhang et al., 2020). Electron donors are pivotal to these bioprocesses (Luo et al., 2019). Although organics can support higher microbial activities, supplementary additions are necessary due to the low availability of organics underground, which increases operational cost (Zhang et al., 2018). Furthermore, biomass yields are larger for heterotrophic processes, which can potentially clog aquifers (Xu et al., 2016). Solubility of Cr(III) can also be enhanced by the formation of organic-Cr(III) complexes (Lai et al., 2016). Microbial Cr(VI) reduction under chemoautotrophic conditions is of interest for practical applications. Gaseous inorganic electron donors, such as hydrogen, can provide electrons for Cr(VI) bio-reduction (Chung et al., 2006). Obviously, the safe usage and storage of such donor gases are important issues. Cr(VI) can be biologically removed by solid elemental sulfur or zerovalent iron (Shi et al., 2019), both of which are engineered materials with poor environmental compatibility. The use of natural materials which provide electrons would make Cr(VI) bio-reduction more sustainable. Hence, Fe(II)-bearing minerals, such as pyrite (FeS_2), mackinawite (FeS), wustite (FeO), and

magnetite (Fe_3O_4) are attractive options for remediation because they occur in abundance in the natural environment (Kantar et al., 2015). Their oxidations can be coupled to abiotic reductive detoxification of pollutants such as chlorinated ethylene, pertechnetate, and Cr(VI) (Cui et al., 1996; Lee et al., 2002; Park et al., 2018; Li et al., 2019; Cai et al., 2019; Wang et al., 2019). Although Cr(VI) bio-reduction by Fe(II)-bearing minerals have been reported (Gan et al., 2019), the performance by pure culture restricts practical applications. Information on microbially mediated Fe(II)-bearing minerals oxidation and Cr(VI) reduction with quantitative identification of biotic and abiotic contributions is still lacking.

This work investigates the bioprocesses of microbial Cr(VI) reduction, supported by Fe(II)-bearing minerals. Both batch and column experiments are conducted. Breakthrough study, analysis of microbial community, quantifications of possible functional genes and proteins, and examination of metabolic intermediates are performed. The main research objectives are: (1) to understand the performance of Fe(II)-bearing minerals dependent Cr(VI) bio-reduction; (2) to distinguish biotic and abiotic contributions to Cr(VI) reduction during these processes; and (3) to reveal the microbial community evolution and associated mechanisms.

2. Materials and methods

2.1. Batch experiment

Four kinds of Fe(II)-bearing minerals, i.e. pyrite, mackinawite, wustite, and

magnetite were commercially purchased from Haoyu Company (Guangdong, China). Table S1 and Fig. S1 in Supporting Information (SI) listed the constituents and structure. The minerals were grounded and sieved to obtain particles of diameter about 1 mm. 5 g amounts of these particles were added to four 250 mL glass bioreactors, which were then sealed with silica gel stoppers and covered by aluminum (Fig. S2a, SI). Each batch bioreactor was inoculated with 50 mL anaerobic consortium obtained from a brewery wastewater treatment facility (organic loading: 5.1 kg chemical oxygen demand (COD)/(m^3·d); hydraulic residence time (HRT): 12 h) and 200 mL synthetic groundwater with ingredients as previously reported (Wang et al., 2018). Cr(VI) was added in the form of $K_2Cr_2O_7$ with initial concentration of 50 mg/L considering Cr(VI) levels in actual contaminated aquifer (Novak et al., 2018). All microbial consortia in bioreactors were acclimated for two months before data collection, then Cr(VI) removals were recorded during 96 h operation to evaluate the performance of the four Fe(II)-bearing minerals. Another three reactors, which were respectively inoculated without minerals, fed with sterilized consortium, and with mackinawite solely added, were also employed as controls. All experiments were conducted at room temperature (22 ± 2 ^oC) and in triplicate.

2.2. Column experiment and breakthrough study

The column comprised a plexiglass cylinder of 25 cm height and 5 cm diameter (Fig. S2b, SI), covered by aluminum foil. A total of 50 g ground shells ($CaCO_3$, 1-3 mm) was added as the inorganic carbon source, supplemented by 50 mL anaerobic consortium and 200 g mackinawite. The left space was filled with quartz sand (1-2

mm) to adjust the porosity. All media were mixed fully in the column. Synthetic Cr(VI)-contaminated groundwater without bicarbonate was upflowed into the column by a peristaltic pump (BT100-1L, Longer, UK). Column operation lasted 180 days, divided into five stages to investigate the influences of groundwater chemistry and hydrodynamics (Table 1). Cr(VI) removal, chemicals in aqueous phase, and the microbial dynamics were monitored at every stage. Solid reaction products, functional genes and proteins were intensively investigated at Stage 5.

Two cylindrical columns (each of 25 cm height and 5 cm diameter) were used for the breakthrough study, with 4 sampling ports evenly distributed along the length of each cylinder. One contained the same constituents as in the column experiment (Biotic column), the other was equipped with only 200 g mackinawite (Abiotic column). Quartz sand was used to pack the columns fully. The flow rate was set with 2 h duration for 1 PV (pore volume). Cr(VI) concentration was continuously recorded.

2.3. Analytical methods

All aqueous samples were ready for analysis after passing through 0.22 μm filters. Concentrations of Cr(VI), nitrate, nitrite, and ammonium were spectrophotometrically monitored using an UV-visible spectrophotometer (UV2300, Shanghai, China) (Zhai et al., 2019). Concentration of dissolved total Cr was determined by means of inductively coupled plasma mass spectrometry (X series, Thermo Fisher, Germany). The limits of quantitation for Cr(VI) and total Cr were 4 μg/L and 0.003 ng/L, respectively. Ion chromatography (Basic IC 792, Metrohm, Switzerland) measured sulfate, sulfite, and thiosulfate. A multifunctional meter

(SevenExcellenceS400, Mettler-Toledo, Switzerland) monitored pH, ORP, and conductivity. Volatile fatty acids (VFAs) in aqueous solution were determined by a gas chromatograph (Agilent 4890, J&W Scientific, USA) equipped with a flame ionization detector. For solid samples, the raw minerals, and resulting precipitates were examined as follows. Elemental content was evaluated using X-ray fluorescence (XRF, F7000, Hitachi, Japan). Components were analyzed by energy dispersive X-ray (EDS) on a scanning electron microscope (SEM) (JEOL JAX-840, Hitachi, Japan). X-ray diffraction (XRD) analysis of the material structures was performed with Cu-Kα (λ = 1.5405 Å) as the radiation source, operated at 40 kV and 200 mA (Rigaku-D/MAX-PC 2500, Rigaku, Japan). X-ray photoelectron spectroscopy (XPS) measurement was undertaken using a Kratos XSAM-800 spectrometer (UK) with a Mg-Kα radiator to determine the valences of responding elements.

2.4. Microbiological analysis

Microbial samples collected at different stages of the column experiment were ultrasonically pretreated. The FastDNA® SPIN Kit for Soil (Qiagen, CA, the USA) was used to extract total genomic DNA of the samples. The DNA was then amplified by PCR (GeneAmp® 9700, ABI, the USA) with primer pair 338F and 806R. Extracted DNA was purified for high-throughput 16S rRNA gene sequencing using MiSeq (Illumina, USA), furnished by Shanghai Majorbio Technology (Shanghai, China). Information on the microbial community was obtained from sequencing data using the method previously described (Zhang et al., 2018). Functional genes involved in S(-II) oxidation (*soxB*) and Cr(VI) reduction (*chrA* and *yieF*) were

quantified using a real-time quantitative PCR (qPCR) detecting system (ABI 7500, Applied Biosystems, the USA), with previously reported primers (Table S2, SI) and procedures (Meyer et al., 2007; He et al., 2011). Cytochrome c falls within a category of specific proteins that can facilitate Fe(II) oxidation through electron transfer (Liu et al., 2012). The content of cytochrome c was measured spectrophotometrically, and normalized to volatile suspended solids (VSS) (Kang et al., 2018; Zhang et al., 2019b).

3. Results and discussion

3.1. Cr(VI) bio-reduction by Fe(II)-bearing minerals

Cr(VI) removal efficiency gradually increased with time in the four batch bioreactors (Fig. 1a), demonstrating the feasibility of Cr(VI) bio-reduction by natural Fe(II)-bearing minerals. After 96 h operation, Cr(VI) removal efficiency ranged from 87.6 ± 1.21% to 98.1 ± 1.21% ($p < 0.05$), with removal rate varying from 0.45 ± 0.03 mg/L·h to 0.54 ± 0.04 mg/L·h ($p < 0.05$). This indicates the advantage of Fe(II)-bearing minerals rather than gaseous electron donors, noting that the Cr(VI) removal rate was only 0.003 mg/L·h with hydrogen as electron donor (Chung et al., 2006). The effectiveness of Fe(II)-bearing minerals as electron donors in supporting Cr(VI) reduction could be attributed to reduced Fe(II) with high reactivity in the minerals (Grabb et al., 2017). Mackinawite performed best out of the minerals considered in this study. It also performed better than a previously employed solid

electron donor, elemental sulfur, which had Cr(VI) removal efficiency of 92.9% in 120 h (Shi et al., 2019), and was comparable to organic electrons, where Cr(VI) removal rate of 0.62 mg/L·h was achieved using acetate (Reddy et al., 2017). Mackinawite has stronger reducing activities with metastable structure (He et al., 2010). Besides Fe(II), reduced S(-II) in mackinawite could also provide supplementary electrons for Cr(VI) reduction. Although pyrite also possesses reduced S species, it resists proton attack under anaerobic conditions with lower bioavailability (Schippers et al., 2002; Bryce et al., 2018), and so was less effective than mackinawite in Cr(VI) bio-reduction.

Cr(VI) removal was also initially detected in the abiotic control (Fig. S3, SI), consistent with previous studies due to superior reducibility of mackinawite (Gong et al., 2017). However, Cr(VI) reduction progressively weakened, as mackinawite was gradually passivated because of the formation of a surface covering of Cr(III) and Fe(III) oxides (Fig. S4, SI). This might hinder the electron transfer process, causing the reaction to retard or even stop, as reported previously (Mullet et al., 2004). Microbial activities could alleviate passivation through partially dissolving the precipitates (Zhong et al., 2017). Cr(VI) was hardly removed in the sterilized control, which excluded any contribution from biomass adsorption. Cr(VI) reduction was retarded as residual organics became exhausted in the inoculum in the control containing a solely anaerobic consortium, suggesting that the electron donor had a critical function in Cr(VI) bio-reduction.

3.2. Long-term Cr(VI) removal under varied chemical and hydrodynamic conditions

Figure 1b showed time series of influent and effluent Cr(VI) concentrations, and Cr(VI) removal efficiency and capacity during 180 d operation in the mackinawite-packed biological column. In Stage 1 (Day 0-50), Cr(VI) was completely removed from the influent with Cr(VI) concentration of 10 mg/L for a HRT of 24 h. In Stage 2 (Day 51-80), when the influent Cr(VI) concentration was increased to 50 mg/L, the Cr(VI) removal efficiency slightly decreased to 94.2 ± 1.52%, whereas the Cr(VI) removal capacity increased from 10.0 g/(m^3·d) at Stage 1 to 47.1 ± 1.16 g/(m^3·d). In Stage 3 (Day 81-107), when the HRT was further shortened to 12 h (influent Cr(VI) concentration of 50 mg/L), an obvious decrease in Cr(VI) removal efficiency to 43.6 ± 1.71% and a slight decrease in Cr(VI) removal capacity to 45.3 ± 9.10 g/(m^3·d) were observed. Similar trends were also reported in abiotic Cr(VI) reduction by pyrite and methane-dependent Cr(VI) bio-reduction (Liu et al., 2015; Lai et al., 2016).

In Stage 4 (Day 108-150), when 10 mg/L NO_3^- was introduced in parallel, with operating conditions the same otherwise as in Stage 2, the Cr(VI) removal efficiency decreased considerably to 23.1 ± 1.22%, with complete removal of nitrate. Cr(VI) removal lagged behind nitrate, as also reported previously (Chung et al., 2006). Given that nitrate is distributed ubiquitously in aquifers, the competitive removals of both Cr(VI) and nitrate confirms that our proposed biosystem could successfully handle co-contaminated groundwater. In Stage 5 (Day151-180), when the operational conditions returned to those of Stage 1, Cr(VI) removal efficiency progressively recovered to 100%. This outcome proved that the proposed biosystem was robust in

resisting fluctuations in groundwater chemistry and hydrodynamics, highlighting its practical applicability.

3.3. Quantification of biotic and abiotic Cr(VI) reductions

Fig. 2a showed Cr(VI) breakthrough curves for different reactive media. In the Abiotic column, structural Fe(II) reduced Cr(VI) chemically, but the passivation by produced iron oxides restricted Cr(VI) removal, and its breakthrough occurred in 33 PV. In the Biotic column with mackinawite, Cr(VI) was removed both chemically and biochemically. Furthermore, the reaction sites of mackinawite could be regenerated through microbial activities, such as secreting acidic metabolites and/or reducing the amount of Fe(III) produced (Gan et al., 2018). Thus, the reaction between Cr(VI) and mackinawite was restored, effectively extending the reaction duration and hence the lifetime of the column, with Cr(VI) penetrating at 168 PV. The longevity of the inoculated column was 5.09 times longer than that of the abiotic one. By fitting the obtained breakthrough curves, biotic and abiotic contributions to Cr(VI) reduction in the Biotic column were calculated to be 76.0 ± 1.12% and 24.1 ± 1.43%, respectively.

Cr(VI) migration in the Biotic column was further investigated. At Port 1 (5 cm from the inlet), rapid breakthrough occurred, whereas migration patterns at the other ports and outlet remained almost the same. The migration rates of the Cr(VI) fronts decreased from Port 1 to the outlet in turn. The Abiotic column also displayed similar behavior (Fig. S5, SI). Using linear regression, the migration rate of the Cr(VI) front in the Biotic column was estimated to be 0.53 ± 0.03 cm/PV (Fig. 2b), a lower figure

than in the Abiotic column (2.08 ± 0.13 cm/PV) (Fig. S7, SI), consistent with previous results (Zhong et al., 2017).

3.4. Reaction products identification and bioprocess elucidation

During the column experiment, the concentration of dissolved total Cr was almost equal to that of Cr(VI) in the effluent (Fig. S6a, SI), implying that precipitation of Cr(VI) reduction products had occurred. Microbes were associated with the precipitates, according to the SEM image (Fig. 3a). EDS analysis suggested that the precipitates contained elemental Cr (Fig. 3b). Distinct characteristic peaks of Cr(III) occurred in the XRD pattern for the precipitates, in the forms of $Cr(OH)_3$ and CrO(OH) (Fig. 3c). Two peaks in the Cr 2p spectrum were evident at 577.6 eV and 587.4 eV from XPS analysis (Fig. 3d), implying that the valence of Cr in the precipitates was +3 (Shi et al., 2019), and confirming that Cr(VI) was reduced to insoluble Cr(III).

Elemental Fe was also detected in the produced precipitates by EDS analysis (Fig. 3b), with characteristic peaks of Fe(III) related to $Fe(OH)_3$ and FeO(OH) displayed in the XRD pattern (Fig. 3c). Fe 2p peaked at 711.7 eV and 725.2 eV in the XPS pattern (Fig. 3e), corresponding to Fe(III) (Tang et al., 2016). No soluble Fe species were detected in the effluent. These results indicated that the structural Fe in mackinawite was oxidized to Fe(III). Sulfate accumulated in the effluent (Fig. 1b), with trace sulfite and undetected thiosulfate (Fig. S6b, SI), which could be derived from oxidation of S(-II) in mackinawite. There was also an S peak visible in the EDS results (Fig. 3b). The S 2p spectrum peaked at 163.4 eV in the XPS pattern,

corresponding to S^0 (Fig. 3e) (Mullet et al., 2004). These intermediates also resulted from oxidation of mackinawite, and they might also act as supplementary electron donors for Cr(VI) bio-reduction (Shi et al., 2019). Although FeS was detected in the feed minerals after reaction, transformation of mackinawite into pyrrhotite was observed (Fig. 3f) (Li et al., 2008). Similar phenomena had also been observed in microbially-driven mineralogical composition of red-gray bauxite and phase transitions of iron sulfides formed by steel microbial corrosion (Laskou et al., 2007; El Mendili et al., 2013).

Considering the observed products and slightly increased solution pH (Fig. S6c, SI), the process of Cr(VI) bio-reduction supported by mackinawite may be expressed by Eq. (1),

$$3CrO_4^{2-} + FeS + 8H_2O \rightarrow Fe^{3+} + 3Cr^{3+} + SO_4^{2-} + 16OH^- \quad (1)$$

Nitrogen loss in aqueous solution occurred once nitrate was introduced (Fig. S6d, SI), with the denitrification reaction expressed by Eq. (2) (Schippers et al., 2002),

$$9NO_3^- + 5FeS + 7H_2O \rightarrow 5Fe^{3+} + 5SO_4^{2-} + 4.5N_2\uparrow + 14OH^- \quad (2)$$

Accumulation of trace ammonium also occurred, with the ammonium production arising from dissimilatory nitrate reduction to ammonium through the following process (Eq. (3)) (Liu et al., 2015),

$$9NO_3^- + 8FeS + 31H_2O \rightarrow 8Fe^{3+} + 8SO_4^{2-} + 9NH_4^+ + 26OH^- \quad (3)$$

3.5. Microbial community evolution and functional gene examination

Microbial richness and diversity increased from Stage 1 to Stage 2 (Fig. S7,

Table S3, SI). Nevertheless, both richness and diversity decreased when either the loading was further enhanced (Stage 3) or co-contaminant nitrate was present (Stage 4). These changes were irreversible, as evidenced by Stage 5 which possessed the lowest richness and diversity, with even the operating conditions and Cr(VI) removal performance the same as in Stage 1. *Deltapotoobacteria* and *Anaerolineae* predominated in all stages at class level (Fig. 4a). *Betaproteobacteria* and *Gammaproteobacteria* gradually accumulated during operation. *Actinobacteria* seemed to be more tolerant to Cr(VI), with highest relative abundance (17.1%) appearing at Stage 3 at the highest Cr(VI) loading.

High relative abundance of *Geobacter* occurred during all stages, at genus level (Fig. 4b). *Geobacter* had well established ability to reduce Cr(VI) (Gong et al., 2018), and so was most likely to be responsible for Cr(VI) removal in the present proposed bio-system. *Anaerolineaceae* accumulated under lower Cr(VI) loadings (Stage 1 and Stage 2) and cooccurrence of Cr(VI) and nitrate (Stage 4). *Anaerolineaceae* could reduce selenate with synthesized selenate reductases (Fakra et al., 2018). It might be also involved in Cr(VI) as the reductases were nonselective, however, its relative abundance decreased at Stage 5. The sulfate-reducing bacterium *Syntrophobacteraceae* enriched progressively during operation, especially in Stage 4, perhaps was stimulated by sulfate produced by mackinawite oxidation (Peng et al., 2018). *Acidovorax*, a reported neutrophilic chemoautotrophic nitrate-reducing Fe(II) iron oxidizer (Pantke et al., 2011), was collectively enriched through the experiment, and might have actively participated in mackinawite oxidation.

qPCR determination showed that *soxB* gene was abundantly present (Fig. 5a), Among sulfur-oxidizing bacteria, *soxB* gene is a representative gene that encodes components of the Sox enzyme system, and presents a widespread pathway by which to oxidize reduced inorganic sulfur compounds (Meyer et al., 2007). This result suggested that S(-II) oxidation in mackinawite could be attributed to the *soxB* gene during microbial metabolic processes. The abundances of two potential Cr(VI) reduction genes *chrA* and *yieF* also increased significantly. Regarding Cr(VI) transport, *ChrA* is responsible for Cr(VI) efflux, and so the *chrA* gene could be related to Cr(VI) resistance in the microbial consortium employed here (He et al., 2018). The transformation of Cr(VI) to Cr(III) was possibly completed through Cr(VI) reductase encoded by the *yieF* gene, which had previously been reported to be involved in Cr(VI) reduction in *Lysinibacillus* (He et al., 2011). Moreover, extracellular Fe(II) oxidation by neutrophilic microorganisms such as *Acidovorax* is realized through an electron transfer pathway formed by cytochrome c components such as MtoA and MtoB (Lu et al., 2013; Shi et al., 2016). The substantial increase in cytochrome c in column experiment was probably associated with oxidation of Fe(II) in mackinawite.

VFAs, possible intermediates in microbial metabolisms, accumulated in Stage 5, with an average concentration of 9.80 ± 1.09 mg/L (Fig. 5b). These metabolites might be derived from reduction of inorganic carbon sources catalyzed by hydrogenases (Khdhiri et al., 2015), with energy supplied from mackinawite oxidation. VFAs could be consumed directly as electron donors for heterotrophic Cr(VI) reducers such as *Geobacter* to detoxify Cr(VI) (Gong et al., 2018). Valerate species accounted for the

majority of residual VFAs, differing from butyrate accumulations mainly in elemental sulfur or zerovalent iron supported biosystems (Shi et al., 2019). Heterotrophs favored small molecule VFAs, which might be directly consumed after synthesis, resulting in lower enrichment (Liu et al., 2016).

3.6. Proposed mechanism and environmental significance

Combining the results of reaction products, microbial community succession, functional genes and intermediate metabolites, a synergistic mechanism between microbial oxidation of mackinawite and Cr(VI) bio-reduction is proposed (Fig. 6). First, autotrophic microorganisms such as *Acidovorax* oxidize mackinawite to Fe(III) and sulfate as the final product and release energy (Pantke et al., 2011). At the same time, the electrons produced reduce inorganic carbon sources to form VFAs as byproducts (Khdhiri et al., 2015). Cr(VI)-reducing functional genus such as *Geobacter* directly reduce Cr(VI) to Cr(III) using VFAs as electron donors (Gong et al., 2018). The upregulated genes are responsible for S oxidation (*soxB*) and Cr(VI) reduction (*chrA*, *yieF*), while cytochrome c performs Fe(II) oxidation (He et al., 2011; Liu et al., 2012). Finally, Cr(III) and Fe(III) precipitate naturally in a near-neutral pH environment.

This study has demonstrated the bioprocesses of microbial Cr(VI) reduction supported by Fe(II)-bearing minerals for the first time (to the authors' knowledge). Batch experiments showed that mackinawite possesses the highest efficiency of the four Fe(II)-bearing minerals considered in Cr(VI) removal. Column experiments lasting 180 d indicated that Cr(VI) concentrations, HRT, and the presence of

additional contaminants such as nitrate all affect removal efficiency. The breakthrough study implied that the biological process accounts for 76.0 ± 1.12% and the abiotic process accounts for 24.1 ± 1.43% of Cr(VI) removal. It also indirectly verified that the combination of biological and chemical processes significantly improves system performance and lifespan. Analyses of microbial communities, related functional genes, proteins, and metabolites suggested that synergy of autotrophic and heterologous microorganisms is critical in Cr(VI) removal. The reduction product Cr(III) would naturally precipitate in groundwater. As an electron donor for Cr(VI) bio-reduction, the oxidation products of mackinawite can precipitate concomitantly as Fe(III) or as harmless sulfate (Veeramani et al., 2013), preventing secondary pollution of groundwater. The co-existence of other metal ions, such as vanadate, with Cr(VI) in natural aquifers should be taken into account when bioremediation based on Fe(II)-bearing minerals is conducted in practice (Zhang et al., 2019a). It should be noted that re-oxidation of produced Cr(III) to Cr(VI) can occur, especially with the presence of oxygen (Apte et al., 2006). Anaerobic condition should be kept for the remediated aquifer and electron donors should be sustainably provided to prevent this re-oxidation phenomenon.

4. Conclusions

In this work, Cr(VI) bio-reduction with Fe(II)-bearing minerals (pyrite, mackinawite, wustite, and magnetite) as inorganic electron donors was evaluated. Batch test indicated that mackinawite (FeS) performed best, with Cr(VI) removal

efficiency of 98.1 ± 1.21% in 96 h and removal rate of 0.54 ± 0.04 mg/L·h. Groundwater chemistry and hydrodynamics influenced Cr(VI) removals in continuous column experiments. Biotic and abiotic contributions of mackinawite to Cr(VI) reduction were 76.0 ± 1.12% and 24.1 ± 1.43%, respectively. The dynamics of microbial communities and functional genes provide evidence for both direct and synergetic mechanisms were involved, as revealed by microbial community dynamics, functional gene abundance and related protein content.

Author Contribution Statement

Jianping Lu: Investigation, **Baogang Zhang**: Conceptualization; Supervision, **Chao He**: Writing - original draft, **Alistair G.L. Borthwick**: Writing - review & editing.

Declaration of interests

The authors declare that they have no known competing financial interests or personal relationships that could have appeared to influence the work reported in this paper.

Acknowledgements

This research work was supported by the National Natural Science Foundation of China (NSFC) (No. 41672237) and Beijing Nova Program (No. Z171100001117082).

References

Apte, A.D., Tare, V., Bose, P., 2006. Extent of oxidation of Cr(III) to Cr(VI) under various conditions pertaining to natural environment. J. Hazard. Mater. 128, 164-174.

Barrera-Diaz, C.E., Lugo-Lugo, V., Bilyeu, B., 2012. A review of chemical, electrochemical and biological methods for aqueous Cr(VI) reduction. J. Hazard. Mater. 223, 1-12.

Bryce, C., Blackwell, N., Schmidt, C., Otte, J., Huang, Y.M., Kleindienst, S., Tomaszewski, E., Schad, M., Warter, V., Peng, C., Byrne, J.M., Kappler, A., 2018. Microbial anaerobic Fe(II) oxidation – Ecology, mechanisms and environmental implications. Environ. Microbiol. 20, 3462-3483.

Cai, W., Fu, F., Zhu, L., Tang, B., 2019. Simultaneous removal of chromium (VI) and phosphate from water using easily separable magnetite/pyrite nanocomposite. J. Alloys Compd. 803, 118-125.

Chebeir, M., Liu, H., 2018. Oxidation of Cr(III)-Fe(III) mixed-phase hydroxides by chlorine: Implications on the control of hexavalent chromium in drinking water. Environ. Sci. Technol. 52, 7663-7670.

Chung, J., Nerenberg, R., Rittmann, B.E., 2006. Bio-reduction of soluble chromate using a hydrogen-based membrane biofilm reactor. Water Res. 40, 1634-1642.

Cui, D., Eriksen, T.E., 1996. Reduction of pertechnetate in solution by heterogeneous electron transfer from Fe(II)-containing geological material. Environ. Sci. Technol. 30, 2263-2269.

El Mendili, Y., Abdelouas, A., El Hajj, H., Bardeaub, J.F., 2013. Phase transitions of iron sulphides formed by steel microbial corrosion. RSC Adv. 3, 26343-26351.

Fakra, S.C., Luef, B., Castelle, C.J., Mullin, S.W., Williams, K.H., Marcus, M.A., Schichnes, D., Banfield, J.F., 2018. Correlative cryogenic spectro-microscopy to

investigate Selenium bioreduction products. Environ. Sci. Technol. 52, 503-512.

Gan, M., Gu, C., Ding, J., Zhu, J., Liu, X., Qiu, G., 2019. Hexavalent chromium remediation based on the synergistic effect between chemoautotrophic bacteria and sulfide minerals. Ecotoxicol. Environ. Saf. 173, 118-130.

Gan, M., Li, J., Sun, S., Cao, Y., Zheng, Z., Zhu, J., Liu, X., Wang, J., Qiu, G., 2018. The enhanced effect of Acidithiobacillus ferrooxidans on pyrite based Cr(VI) reduction. Chem. Eng. J. 341, 27-36.

Gang, H., Xiao, C., Xiao, Y., Yan, W., Bai, R., Ding, R., Yang, Z., Zhao, F., 2019. Proteomic analysis of the reduction and resistance mechanisms of S*hewanella oneidensis* MR-1 under long-term hexavalent chromium stress. Environ. Int. 127, 94-102.

Gong, Y., Werth, C.J., He, Y., Su, Y., Zhang, Y., Zhou, X., 2018. Intracellular versus extracellular accumulation of hexavalent chromium reduction products by Geobacter sulfurreducens PCA. Environ. Pollut. 240, 485-492.

Gong, Y., Gai, L., Tang, J., Fu, J., Wang, Q., Zeng, E.Y., 2017. Reduction of Cr(VI) in simulated groundwater by FeS-coated iron magnetic nanoparticles. Sci. Total Environ. 595, 743-751.

Grabb, K.C., Buchwald, C., Hansel, C.M., Wankel, S.D., 2017. A dual nitrite isotopic investigation of chemodenitrification by mineral-associated Fe(II) and its production of nitrous oxide. Geochim. Cosmochimi. Acta 196, 388-402.

Hausladen, D.M., Alexander-Ozinskas, A., McClain, C., Fendorf, S., 2018. Hexavalent chromium sources and distribution in California groundwater.

Environ. Sci. Technol. 52, 8242-8251.

He, M., Li, X., Liu, H., Miller, S.J., Wang, G., Rensing, C., 2011. Characterization and genomic analysis of a highly chromate resistant and reducing bacterial strain *Lysinibacillus fusiformis* ZC1. J. Hazard. Mater. 185, 682-688.

He, Y., Dong, L., Zhou, S., Jia, Y., Gu, R., Bai, Q., Gao, J., Li, Y., Xiao, H., 2018. Chromium resistance characteristics of Cr(VI) resistance genes *ChrA* and *ChrB* in *Serratia sp.* S2. Ecotoxicol. Environ. Saf. 157, 417-423.

He, Y.T., Wilson, J.T., Wilkin, R.T., 2010. Impact of iron sulfide transformation on trichloroethylene degradation. Geochim. Cosmochim. Acta 74, 2025-2039.

Huang, D., Wang, G., Shi, Z., Li, Z., Kang, F., Liu, F., 2017. Removal of hexavalent chromium in natural groundwater using activated carbon and cast iron combined system. J. Cleaner Prod. 165, 667-676.

Kang, D., Lin, Q., Xu, D., Hu, Q., Li, Y., Ding, A., Zhang, M., Zheng, P., 2018. Color characterization of anammox granular sludge: Chromogenic substance, microbial succession and state indication. Sci. Total Environ. 642, 1320-1327.

Kantar, C., Ari, C., Keskin, S., Dogaroglu, Z.G., Karadeniz, A., Alten, A., 2015. Cr(VI) removal from aqueous systems using pyrite as the reducing agent: Batch, spectroscopic and column experiments. J. Contam. Hydrol. 174, 28-38.

Khdhiri, M., Hesse, L., Popa, M.E., Quiza, L., Lalonde, I., Meredith, L.K., Röckmann, T., Constant, P., 2015. Soil carbon content and relative abundance of high affinity H_2-oxidizing bacteria predict atmospheric H_2 soil uptake activity better than soil microbial community composition. Soil Biol. Biochem. 85, 1-9.

Lai, C.Y., Zhong, L., Zhang, Y., Chen, J.X., Wen, L.L., Shi, L.D., Sun, Y.P., Ma, F., Rittmann, B.E., Zhou, C., Tang, Y., Zheng, P., Zhao, H.P., 2016. Bioreduction of chromate in a methane-based membrane biofilm reactor. Environ. Sci. Technol. 50, 5832-5839.

Laskou, M., Economou-Eliopoulos, M., 2007. The role of microorganisms on the mineralogical and geochemical characteristics of the Parnassos-Ghiona bauxite deposits, Greece. J. Geochem. Explor. 93, 67-77.

Lee, W., Batchelor, B., 2002. Abiotic reductive dechlorination of chlorinated ethylenes by iron-bearing soil minerals. 1. Pyrite and magnetite. Environ. Sci. Technol. 36, 5147-5154.

Li, Y., Liang, J., Yang, Z., Wang, H., Liu, Y., 2019. Reduction and immobilization of hexavalent chromium in chromite ore processing residue using amorphous FeS_2. Sci. Total Environ. 658, 315-323.

Li, Y., van Santen, R.A., Weber, Th., 2008. High-temperatureFeS-FeS_2 solid-state transitions: Reactions of solid mackinawite with gaseous H_2S. J. Solid State Chem. 181, 3151-3162.

Liu, H., Zhang, B., Xing, Y., Hao, L., 2016. Behavior of dissolved organic carbon sources on the microbial reduction and precipitation of vanadium (V) in groundwater. RSC Adv. 6, 97253-97258.

Liu, J., Huang, K., Xie, K., Yang, Y., Liu, H., 2016. An ecological new approach for treating Cr(VI)-containing industrial wastewater: Photochemical reduction. Water Res. 93, 187-194.

Liu, J., Wang, Z., Belchik, S.M., Edwards, M.J., Liu, C., Kennedy, D.W., Merkley, E.D., Lipton, M.S., Butt, J.N., Richardson, D.J., Zachara, J.M., Fredrickson, J.K., Rosso, K.M., Shi, L., 2012. Identification and characterization of MtoA: a decaheme c-type cytochrome of the neutrophilic Fe(II)-oxidizing bacterium *Sideroxydans lithotrophicus* ES-1. Front. Microbiol. 3, 37.

Liu, Y., Zhang, B., Tian, C., Feng, C., Wang, Z., Cheng, M., Hu, W., 2015. Optimization of enhanced bioelectrical reactor with electricity from microbial fuel cells for groundwater nitrate removal. Environ. Technol. 37, 1008-1017.

Liu, Y., Mou, H., Chen, L., Mirza, Z.A., Liu, L., 2015. Cr(VI)-contaminated groundwater remediation with simulated permeable reactive barrier (PRB) filled with natural pyrite as reactive material: environmental factors and effectiveness. J. Hazard. Mater. 298, 83-90.

Lu, S., Chourey, K., Reiche, M., Nietzsche, S., Shah, M.B., Neu, T.R., Hettich, R.L., Küsel, K., 2013. Insights into the structure and metabolic function of microbes that shape pelagic iron-rich aggregates (“iron snow”). Appl. Environ. Microb. 79, 4272-4281.

Luo, J.H., Wua, M., Liu, J., Qian, G., Yuan, Z., Guo, J., 2019. Microbial chromate reduction coupled with anaerobic oxidation of methane in a membrane biofilm reactor. Environ. Int. 130, 104926.

Meyer, B., Imhoff, J.F., Kuever, J., 2007. Molecular analysis of the distribution and phylogeny of the *soxB* gene among sulfur-oxidizing bacteria-evolution of the Sox sulfur oxidation enzyme system. Environ Microbiol. 9, 2957-2977.

Mullet, M., Boursiquot, S., Ehrhardt, J.J., 2004. Removal of hexavalent chromium from solutions by mackinawite, tetragonal FeS. Colloids Surf., A 244, 77-85.

Novak, M., Sebek, O., Chrastny, V., Hellerich, L.A., Andronikov, A., Martinkova, E., Farkas, J., Pacherova, P., Curik, J., Stepanova, M., Prechova, E., Houskova, M., Zoulkova, V., Veselovsky, F., Svobodova, I., Janotova, P., Komarek, A., 2018. Comparison of delta(CrCr)-Cr-53(VI) values of contaminated groundwater at two industrial sites in the eastern US with contrasting availability of reducing agents. Chem. Geol. 481, 74-84.

Pantke, C., Obst, M., Benzerara, K., Morin, G., Ona-Nguema, G., Dippon, U., Kappler, A., 2011. Green rust formation during Fe(II) oxidation by the nitrate-reducing *Acidovorax sp*. strain BoFeN1. Environ. Sci. Technol. 46, 1439-1446.

Park, M., Park, J., Kang, J., Han, Y.S., Jeong, H.Y., 2018. Removal of hexavalent chromium using mackinawite (FeS)-coated sand. J. Hazard. Mater. 360, 17-23.

Peng, W., Li, X., Liu, T., Liu, Y., Ren, J., Liang, D., Fan, W., 2018. Biostabilization of cadmium contaminated sediments using indigenous sulfate reducing bacteria: Efficiency and process. Chemosphere 201, 697-707.

Qian, J., Zhou, J., Wang, L., Wei, L., Li, Q., Wang, D., Wang, Q., 2017. Direct Cr(VI) bio-reduction with organics as electron donor by anaerobic sludge. Chem. Eng. J. 309, 330-338.

Reddy, G.K.K., Nancharaiah, Y.V., 2017. Sustainable bioreduction of toxic levels of chromate in a denitrifying granular sludge reactor. Environ. Sci. Pollut. Res. 25, 1969-1979.

Schippers, A., Jørgensen, B.B., 2002. Biogeochemistry of pyrite and iron sulfide oxidation in marine sediments. Geochim. Cosmochim. Acta 66, 85-92.

Shi, J., Zhang, B., Qiu, R., Lai, C., Jiang, Y., He, C., Guo, J., 2019. Microbial chromate reduction coupled to anaerobic oxidation of elemental sulfur or zerovalent iron. Environ. Sci. Technol. 53, 3198-3207.

Shi, L., Dong, H., Reguera, G., Beyenal, H., Lu, A., Liu, J., Yu, H.Q., Fredrickson, J.K., 2016. Extracellular electron transfer mechanisms between microorganisms and minerals. Nat. Rev. Microb. 14, 651-662.

Tang, J., Huang, Y., Gong, Y., Lyu, H., Wang, Q., Ma, J., 2016. Preparation of a novel graphene oxide/Fe-Mn composite and its application for aqueous Hg(II) removal. J. Hazard. Mater. 316, 151-158.

Veeramani, H., Scheinost, A.C., Monsegue, N., Qafoku, N.P., Kukkadapu, R., Newville, M., Lanzirotti, A., Pruden, A., Murayama, M., Hochella, M.F., 2013. Abiotic reductive immobilization of U(VI) by biogenic mackinawite. Environ. Sci. Technol. 47, 2361-2369.

Wang, S., Zhang, B., Diao, M., Shi, J., Jiang, Y., Cheng, Y., Liu, H., 2018. Enhancement of synchronous bio-reductions of vanadium (V) and chromium (VI) by mixed anaerobic culture. Environ. Pollut. 242, 249-256.

Wang, T., Qian, T., Huo, L., Li, Y., Zhao, D., 2019. Immobilization of hexavalent chromium in soil and groundwater using synthetic pyrite particles. Environ. Pollut. 255, 112992.

Wang, W., Zhang, B., Liu, Q., Du, P., Liu, W., He, Z., 2018. Biosynthesis of palladium

nanoparticles using *Shewanella loihica* PV-4 for excellent catalytic reduction of chromium (VI). Environ. Sci.: Nano 5, 730-739.

Xu, J.H., He, S.B., Wu, S.Q., Huang, J.C., Zhou, W.L., Chen, X.C., 2016. Effects of HRT and water temperature on nitrogen removal in autotrophic gravel filter. Chemosphere 147, 203-209.

Zhai, S., Zhao, Y., Ji, M., Qi, W., 2019. A dicyclic-type electrode-based biofilm reactor for simultaneous nitrate and Cr(VI) reduction. Bioprocess Biosyst. Eng. 42, 167-172.

Zhang, B., Cheng, Y., Shi, J., Xing, X., Zhu, Y., Xu, N., Xia, J., Borthwick, A.G.L., 2019a. Insights into interactions between vanadium (V) bio-reduction and pentachlorophenol dechlorination in synthetic groundwater. Chem. Eng. J. 375, 121965.

Zhang, B., Feng, C., Ni, J., Zhang, J., Huang, W., 2012. Simultaneous reduction of vanadium (V) and chromium (VI) with enhanced energy recovery based on microbial fuel cell technology. J. Power Sources 204, 34-39.

Zhang, B., Qiu, R., Lu, L., Chen, X., He, C., Lu, J., Ren, Z.J., 2018. Autotrophic vanadium (V) bioreduction in groundwater by elemental sulfur and zerovalent iron. Environ. Sci. Technol. 52, 7434-7442.

Zhang, B., Wang, S., Diao, M., Fu, J., Xie, M., Shi, J., Liu, Z., Jiang, Y., Cao, X., Borthwick, A.G.L., 2019b. Microbial community responses to vanadium distributions in mining geological environments and bioremediation assessment. J. Geophys. Res.: Biogeosci. 124, 601-615.

Zhang, B., Wang, Z., Shi, J., Dong, H., 2020. Sulfur-based mixotrophic bio-reduction for efficient removal of chromium (VI) in groundwater. Geochim. Cosmochim. Acta 268, 296–309.

Zhong, J., Yin, W., Li, Y., Li, P., Wu, J., Jiang, G., Gu, J., Liang, H., 2017. Column study of enhanced Cr(VI) removal and longevity by coupled abiotic and biotic processes using Fe^0 and mixed anaerobic culture. Water Res. 122, 536-544.

Table 1. Operating conditions and corresponding Cr(VI) removal performance for each stage in column experiment.

Stage	Period (d)	HRT (h)	Initial Cr(VI) (mg/L)	Initial nitrate (mg/L)	Cr(VI) removal efficiency (%)	Cr(VI) removal capacity ($g/m^3 \cdot d$)
1	0-50	24	10	0	100	10
2	51-80	24	50	0	94.2 ± 1.52	47.1 ± 1.16
3	81-107	12	50	0	43.6 ± 1.71	45.3 ± 9.10
4	108-150	24	50	10	23.1 ± 1.22	11.4 ± 3.63
5	151-180	24	10	0	100	10

Figure captions.

Fig. 1. Cr(VI) removal performance in batch and column experiments. (a) Temporal variations in Cr(VI) removal efficiency in three continuous operating cycles after two-month domestication in batch bioreactors fed with different Fe(II)-bearing minerals. Each cycle lasts 96 h. (b) Time profiles of Cr(VI) and NO_3^- in influent, Cr(VI), NO_3^-, SO_4^{2-} in effluent, and corresponding Cr(VI), NO_3^- removal efficiencies and capacities in mackinawite packed inoculated column during 180 d operation.

Fig. 2. Cr(VI) breakthrough curves in Biotic column and Abiotic column. (a) Effluent Cr(VI) concentration in both columns and Cr(VI) concentrations at different elevations along the Biotic column; (b) Linear regression equation for Cr(VI) migration. Biotic column is equipped with mackinawite and inoculated with anaerobic consortium. Abiotic column is packed solely with mackinawite, and the left space in both columns is filled with quartz sand.

Fig. 3. Physicochemical characterization of reaction products and mackinawite in the column experiment. (a) SEM image of microbes and produced precipitates; (b) EDS pattern of the precipitates; (c) XRD pattern of the precipitates; (d) Cr 2p spectrum for the precipitates obtained using XPS analysis; (e) XPS spectra of Fe 2p and S 2p for the precipitates; (f) XRD patterns of mackinawite before and after reaction.

Fig. 4. Phylogenetic profiling of biomass in the inoculated column packed by mackinawite during 180 d operation at (a) class and (b) genus levels.

Fig. 5. Contents of functional genes, related proteins, and accumulated intermediate metabolites in Stage 5 of the column experiment. (a) Abundance of genes involved in S(-II) oxidation, Cr(VI) reduction, and content of cytochrome c; (b) Mean concentrations of residual VFAs.

Fig. 6. Proposed pathways of microbial Cr(VI) reduction supported by mackinawite.

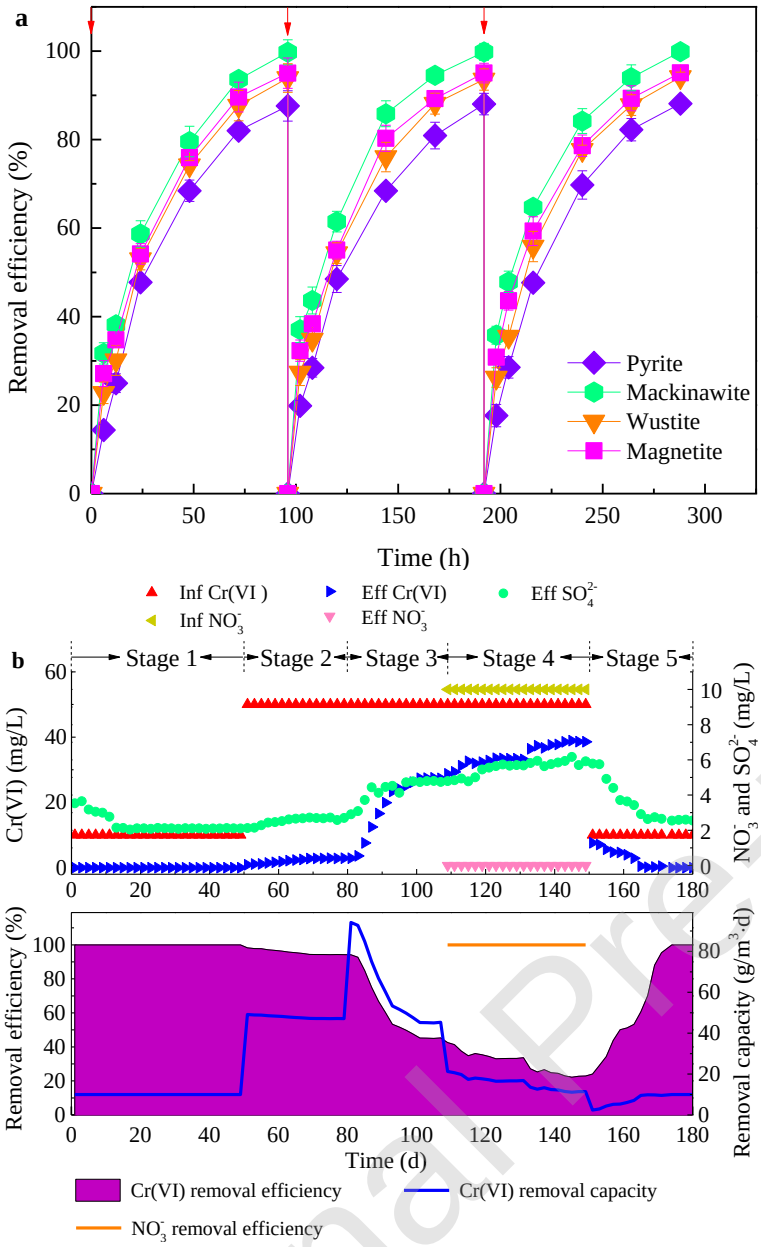

Fig. 1. Cr(VI) removal performance in batch and column experiments. (a) Temporal variations in Cr(VI) removal efficiency in three continuous operating cycles after two-month domestication in batch bioreactors fed with different Fe(II)-bearing minerals. Each cycle lasts 96 h. (b) Time profiles of Cr(VI) and NO_3^- in influent, Cr(VI), NO_3^-, SO_4^{2-} in effluent, and corresponding Cr(VI), NO_3^- removal efficiencies and capacities in mackinawite packed inoculated column during 180 d operation.

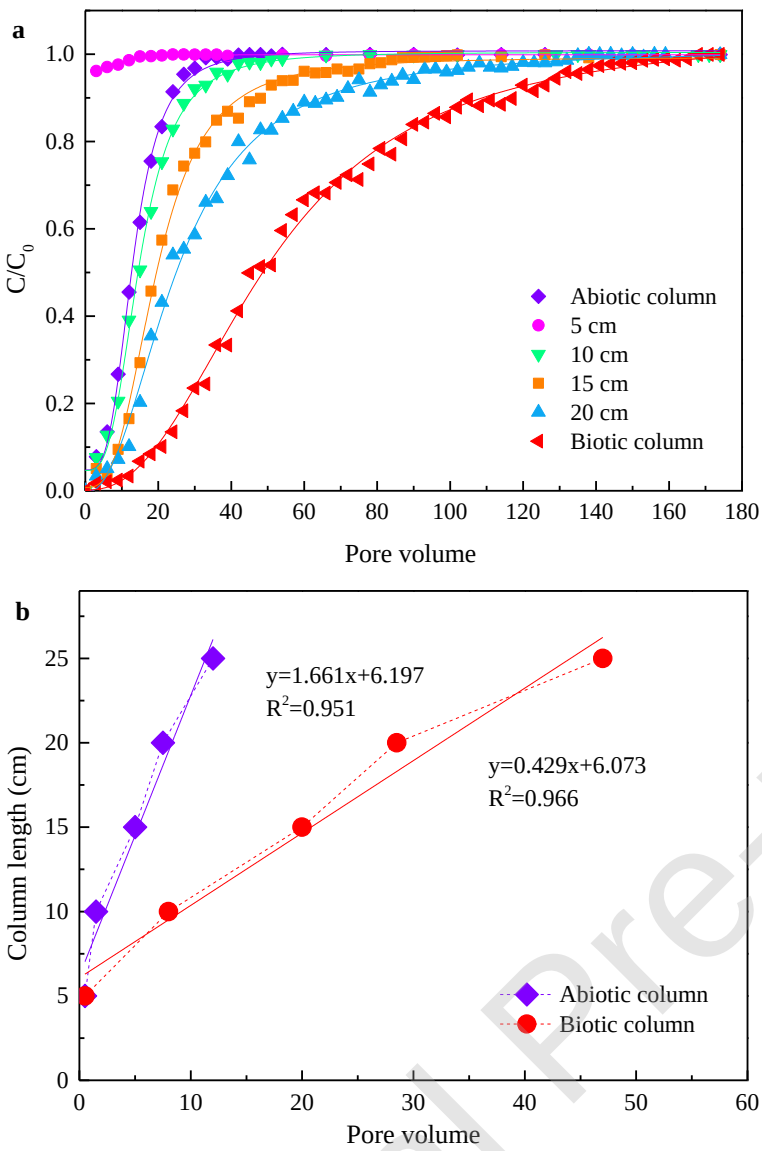

Fig. 2. Cr(VI) breakthrough curves in Biotic column and Abiotic column. (a) Effluent Cr(VI) concentration in both columns and Cr(VI) concentrations at different elevations along the Biotic column; (b) Linear regression equation for Cr(VI) migration. Biotic column is equipped with mackinawite and inoculated with anaerobic consortium. Abiotic column is packed solely with mackinawite, and the left space in both columns is filled with quartz sand.

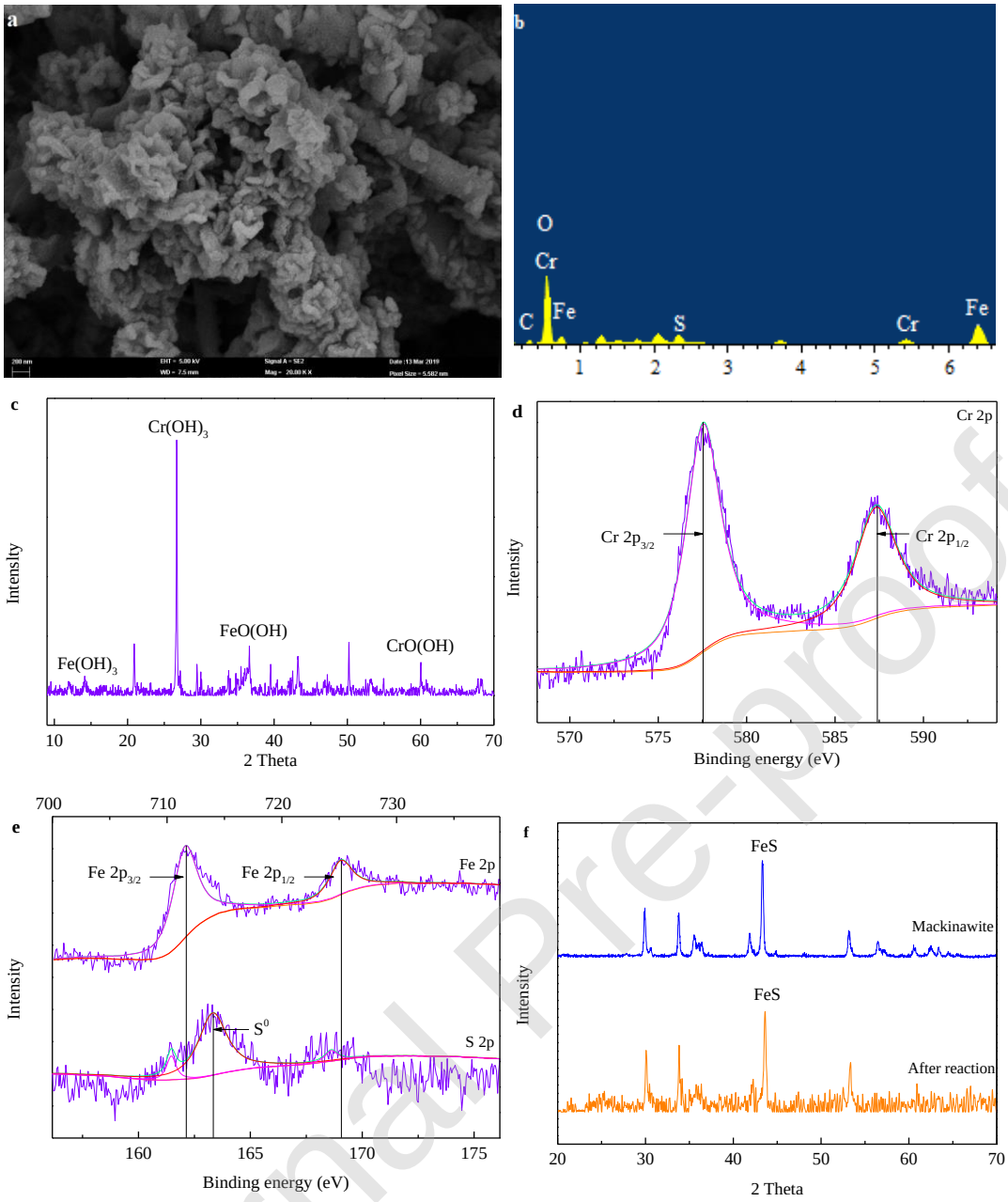

Fig. 3. Physicochemical characterization of reaction products and mackinawite in the column experiment. (a) SEM image of microbes and produced precipitates; (b) EDS pattern of the precipitates; (c) XRD pattern of the precipitates; (d) Cr 2p spectrum for the precipitates obtained using XPS analysis; (e) XPS spectra of Fe 2p and S 2p for the precipitates; (f) XRD patterns of mackinawite before and after reaction.

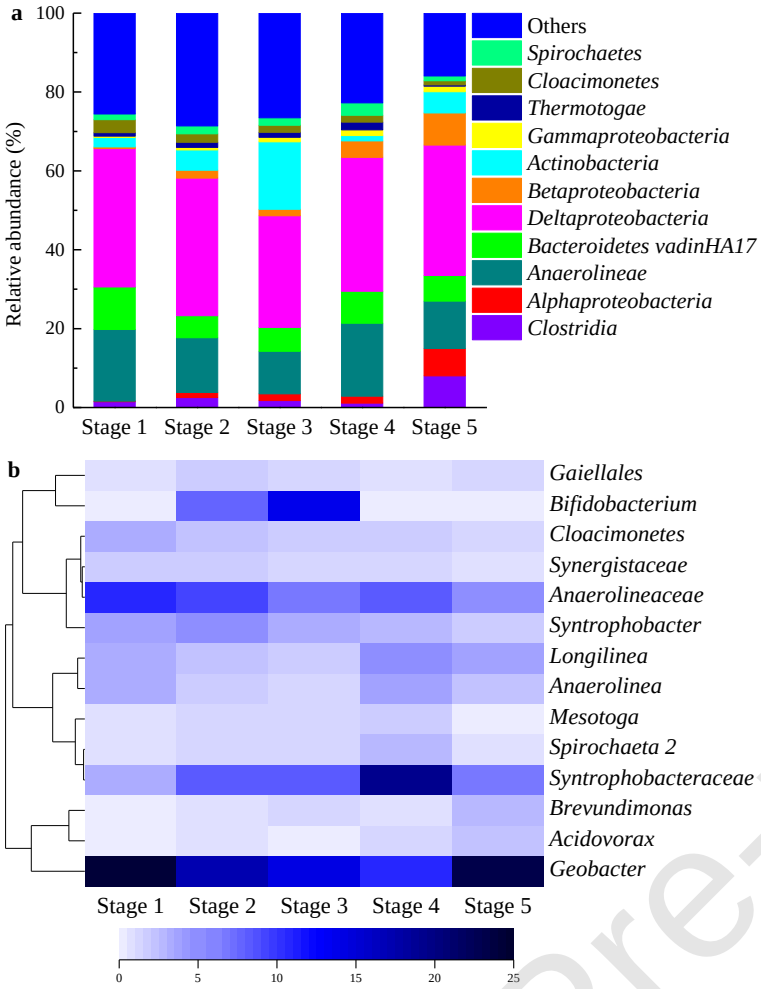

Fig. 4. Phylogenetic profiling of biomass in the inoculated column packed by mackinawite during 180 d operation at (a) class and (b) genus levels.

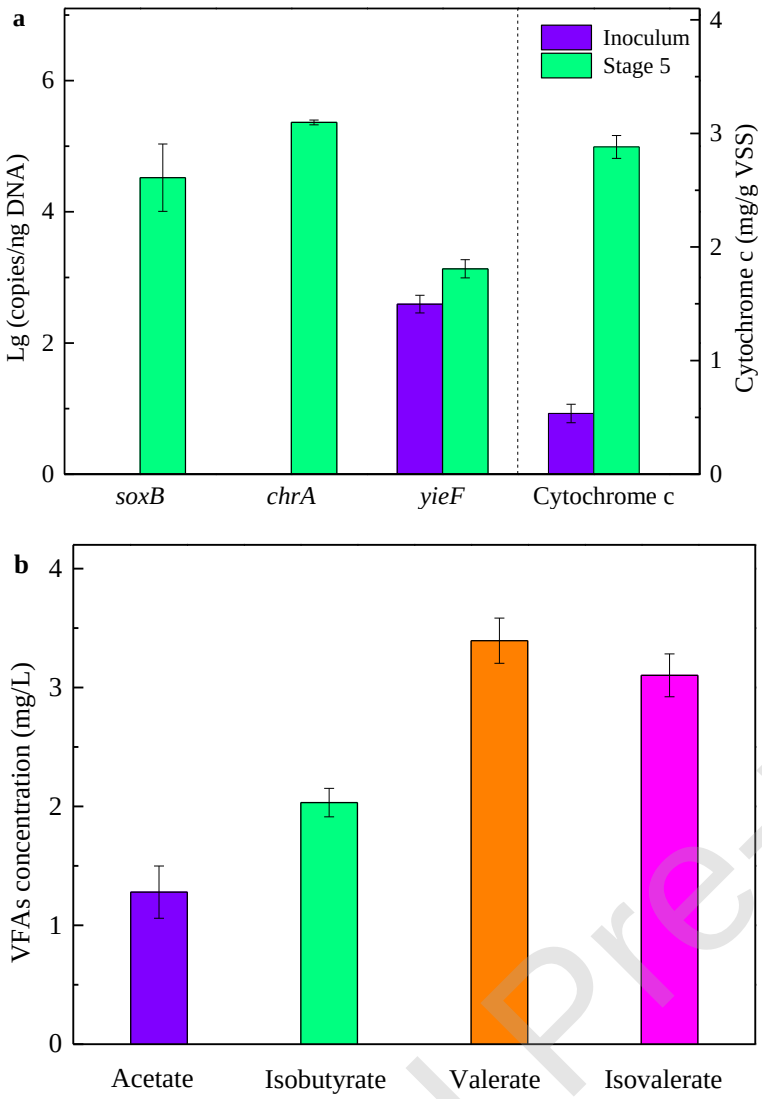

Fig. 5. Contents of functional genes, related proteins, and accumulated intermediate metabolites in Stage 5 of the column experiment. (a) Abundance of genes involved in S(-II) oxidation, Cr(VI) reduction, and content of cytochrome c; (b) Mean concentrations of residual VFAs.

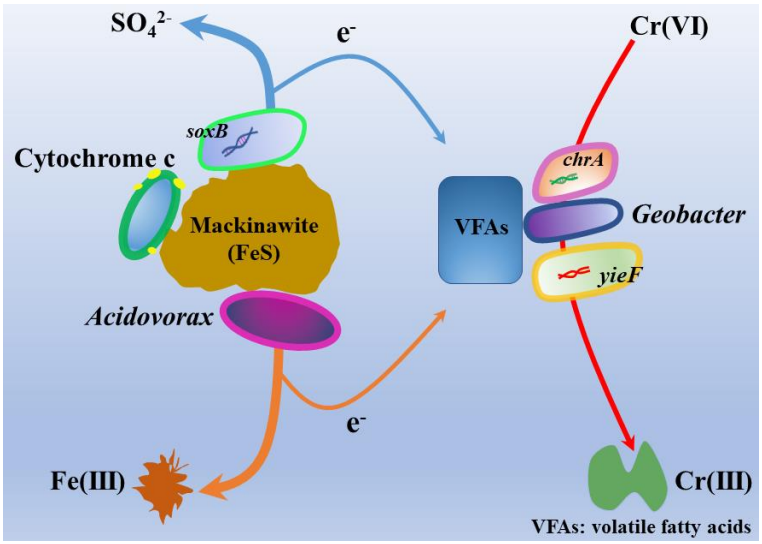

Fig. 6. Proposed pathways of microbial Cr(VI) reduction supported by mackinawite.